



Immobilization of silver nanoparticles at varying concentrations on segments of polyvinyl chloride manufactured endotracheal tubes

Yesenia Andrea Murillo Arias^a, René Ramírez García^b, Marco Antonio González Agudelo^c, Nathalia Marín-Pareja^d, Claudia Patricia Ossa Orozco^{e,*}

^a Grupo de Investigación en Biomateriales, Programa de Bioingeniería, Facultad de Ingeniería, Universidad de Antioquia, Medellín, Colombia

^b Grupo de Investigación Ciencia de los Animales INCA-CES, Universidad CES, Medellín, Colombia

^c Grupo de Investigación en Cuidado Crítico, Universidad Pontificia Bolivariana, Medellín, Colombia

^d Grupo de Investigación en Gestión y Aplicación de la Ciencia y la Tecnología - GIGAT, Tecnoparque Medellín SENA, Medellín, Colombia

^e Grupo de Investigación en Biomateriales, Programa de Bioingeniería, Facultad de Ingeniería, Universidad de Antioquia, Medellín, Colombia

ARTICLE INFO

Keywords:

Endotracheal tubes

Polyvinyl chloride PVC

Silver nanoparticles, antimicrobial, properties

ABSTRACT

Ventilator-associated pneumonia (VAP) remains a significant challenge in intensive care units, representing a primary medical device-associated infection with alarming incidence rates. Patients undergoing mechanical ventilation are particularly vulnerable to VAP due to bacterial accumulation on the endotracheal tube cuff, which can lead to biofilm formation and subsequent migration into the lower respiratory tract, resulting in pneumonia. Currently, various strategies are being explored to mitigate VAP incidence. These approaches encompass innovations in endotracheal tube design, tracheal secretion aspiration systems, material surface modifications, and others. However, a fully effective solution to prevent biofilm formation not yet been developed. Despite ongoing efforts to address VAP through innovations in endotracheal tube design and other preventive measures, a comprehensive solution to effectively prevent biofilm formation has remained elusive. In this study, we have researched the potential of surface modification processes to mitigate bacterial colonization on endotracheal tubes manufactured from polyvinyl chloride (PVC). Specifically, we explored the introduction of silver nanoparticles (AgNPs) at varying concentrations as a strategy to prevent bacterial adherence and biofilm formation. We successfully validated the chemical modification of the surface and subsequent nanoparticle immobilization. This result was accomplished by scrutinizing physicochemical alterations through wetting studies, Fourier-transform infrared spectroscopy (FTIR), and scanning electron microscopy (SEM). Through examination of physicochemical alterations using Fourier-transform infrared spectroscopy (FTIR), wetting studies, and scanning electron microscopy (SEM), we successfully validated the efficacy of the surface modification process proposed and confirmed the immobilization of AgNPs. We conducted mechanical strength assays, revealing that the surface modification process with silver nanoparticles did not compromise the mechanical integrity of the material. Additionally, we conducted antimicrobial efficacy and *in vitro* cytotoxicity assessments of the modified endotracheal tubes. Our findings indicate that the material modified with a 100 % concentration of silver nanoparticles exhibited promising results in reducing bacterial colonization, particularly against *Klebsiella pneumoniae* and *Pseudomonas aeruginosa* strains. It is worth mentioning that we observed no cytotoxic effects on L929 cells, underscoring the safety profile of the modified material for potential clinical application. In conclusion, our study highlights the potential of surface modification with silver nanoparticles as a promising strategy to mitigate bacterial colonization on endotracheal tubes and reduce the risk of VAP in mechanically ventilated patients. These findings contribute to ongoing efforts to enhance patient safety and improve outcomes in critical care settings. Further research and clinical trials are warranted to validate the effectiveness and long-term benefits of this innovative approach in preventing VAP and minimizing associated morbidity and mortality.

* Corresponding author.

E-mail addresses: yesenia.murillo@udea.edu.co (Y.A.M. Arias), framirez@ces.edu.co (R.R. García), marcoantonio.gonzalez@upb.edu.co (M.A.G. Agudelo), nmarinp@sena.edu.co (N. Marín-Pareja), claudia.ossa@udea.edu.co (C.P.O. Orozco).

<https://doi.org/10.1016/j.mtcomm.2024.110109>

Received 6 March 2024; Received in revised form 5 August 2024; Accepted 10 August 2024

Available online 12 August 2024

2352-4928/© 2024 The Author(s). Published by Elsevier Ltd. This is an open access article under the CC BY-NC-ND license (<http://creativecommons.org/licenses/by-nc-nd/4.0/>).

1. Introduction

The endotracheal tube is a medical device used for intubating patients requiring general anesthesia or invasive mechanical ventilation in cases of respiratory failure. Ventilator-associated pneumonia (VAP) can be developed after 48 hours of mechanical ventilation initiation. This healthcare-associated infection occurs in 17–37 % of ventilated patients, contributing to increase direct and indirect mortality, extended hospital stays, augmented antibiotic use, bacterial resistance, and healthcare costs [1]. Microorganisms colonizing the oropharynx and glottis can migrate into the lower airways through overflow or form a biofilm within the endotracheal tube, shielding themselves from antibiotics and facilitating lung infections in these patients [1].

During mechanical ventilation, respiratory secretions aggregate on the endotracheal tube cuff, research indicates that these secretions can migrate to the lower airways, causing pneumonia. The consequences of microaspiration depend on aspirate volume, the presence of infectious agents, their virulence, and the health status of host. In the lungs, inflammatory defense mechanisms activate, if insufficient, pneumonia can lead to sepsis, hypoxemia, potential multi-organ failure, and eventual death. The gold standard for VAP diagnosis involves lung biopsies. Due to invasiveness, temporal, clinical, laboratory, and microbiological criteria have been established following guidelines from the Infectious Diseases Society of America [2,3]. VAP can be caused by various pathogens -bacteria, viruses, and fungi- individually or in a polymicrobial context. Among these are aerobic gram-negative bacilli like *Escherichia coli*, *Klebsiella pneumoniae*, *Enterobacter spp*, *Pseudomonas aeruginosa*, *Acinetobacter spp*, and gram-positive cocci such as Methicillin-resistant *Staphylococcus aureus* (MRSA), *Streptococcus spp* [3].

Efforts to prevent VAP have led to safety care bundles, but VAP incidence remains. Preventive strategies against bacterial adhesion and biofilm formation have not entirely curbed the migration of microorganisms into the lungs, nor have the studies and modifications of these medical devices fully addressed the issue [4–6]. Nonetheless, surface modification with antimicrobial agents is a promising contemporary approach to inhibit bacterial colonization on endotracheal tubes [7,8].

Currently, endotracheal tubes are manufactured from transparent materials, including polyvinyl chloride (PVC), silicone, and polyurethane [7,9,10]. The PVC is used in medical devices fabrication due to this material has gloss, transparency, chemical resistance, wear resistance, flexibility, and it is possible sterilize by steam, ethylene oxide ETO, or high energy irradiation [11]. PVC requires stabilizers additives and plasticizers to prevent thermal degradation during manufactured processes of medical devices and they are essential to conserve the mechanical performance; these additives does not impede biofilm formation; due to that it is necessary to use biocide additives in PVC formulations [12].

When altering the surface properties of materials that come into contact with human tissues to impart antibacterial properties, the material must exhibit characteristics such as low adherence and hydrophobicity. This characteristic is particularly relevant, as hydrophilic bacteria tend to adhere more to hydrophilic surfaces due to their capacity to absorb the surrounding aqueous environment. Thus, the more hydrophobic the material, the less these microorganisms adhere to the surface [13,14]. Over the last decades, silver nanoparticles (AgNPs) have gained attention for their exceptional physicochemical properties and powerful biological activities, rendering them versatile in numerous fields. They exhibit a broad antimicrobial spectrum against various pathogens, including bacteria and fungi such as *Salmonella enterica*, *Staphylococcus spp*, and *Pseudomonas aeruginosa*. Consequently, AgNPs have been employed to confer antibacterial properties to materials lacking them [2,15].

Previous studies have reported the antibacterial effect of PVC-based materials incorporating AgNPs through casting, significant reductions in bacterial growth were observed, confirming antibacterial efficiency [16, 17]. Moreover, Daengngam et al. immobilized AgNPs onto the surface of

a PVC endotracheal tube through immersion in an aqueous solution containing silver nitrate [1]. Wang et al. [18] fabricated a chitosan-AgNPs-gelatin nanocomposite coating on PVC endotracheal tubes, they concluded that this modification improved the antibacterial surface without affect the mechanical properties and present no-toxic behavior. In other research, PVC endotracheal tubes were coated with a double-network hydrogel with addition of silver using an in-situ photoinitiation method, this material exhibited excellent antibacterial performance against methicillin-resistant *Staphylococcus aureus* (MRSA) and *Pseudomonas aeruginosa*, common bacteria in patients staying in intensive care units [19]. Other studies have reported modifications to PVC by adding AgNPs to the surface of polymer, using techniques such as electrospinning, vapor coating, ion implantation, or spray deposition, among others. However, these methods tend to be expensive and require larger quantities of nanoparticles, potentially affecting the transparency of the modified material [16]. There is a report using coating silver nitrate on endotracheal tubes as good strategy to prevent bacterial colonization, however silver nitrate (AgNO_3) has been associated with an increased risk of skin irritation and chemical burns in patients in contact with medical devices modified with AgNO_3 [20]. Currently there is no ideal material for the manufacture of an endotracheal tubes that prevents biofilm formation, which is the main accepted mechanism to produce VAP. Therefore, to study an option to enhance the surface behavior of PVC endotracheal tubes by adding AgNPs is the innovation of this study.

In this study, we analyzed the influence of surface modification processes on segments of endotracheal tubes manufactured from the biocompatible polymer polyvinyl chloride (PVC). We employed a chemical method for immobilizing chemically synthesized silver nanoparticles (AgNPs) at three different concentrations: 100 % (mother solution: refers to synthesized solution), 75 %, and 50 %. The study aimed to explore the resulting physicochemical and biological properties, as well as the antimicrobial capability of the medical-grade PVC modified material.

2. Materials and methods

2.1. Synthesis of silver nanoparticles (AgNPs)

Silver nanoparticles (AgNPs) were synthesized through chemical reduction, following modifications to the protocol by Cuervo et al. [21]. Silver nitrate (AgNO_3) of 100 % purity (Pan Reac Appli Chem ITW reagents) served as the precursor agent. In comparison, trisodium citrate dihydrate ($\text{Na}_3\text{C}_6\text{H}_5\text{O}_7 \times 2 \text{H}_2\text{O}$) with 99 % purity (Pan Reac Appli Chem ITW reagents) was used as the reducing agent. Initially distilled water was heated to 94 °C with magnetic stirring at 200 rpm. Once the water reached the desired temperature, a 0.1 M silver nitrate solution was added with continuous stirring for 10 minutes. Subsequently, a 1 % trisodium citrate solution was added dropwise via burette to the prepared solution. A yellow color change indicated the endpoint. After completing the dropwise addition, the solution was stirred for 3 minutes, removed from heat, and transferred to a reverse water bath to halt the reaction.

2.2. Characterization of AgNPs

The silver nanoparticles obtained were characterized using ultraviolet-visible (UV-Vis) spectrophotometry (UV-VIS MAPADA 3200PC, Mapada Instrument), scanning wavelengths between 300 and 600 nm, using distilled water as a blank. Dynamic light scattering (DLS) analysis (Gama Zetasizer Advance, Malvern Panalytical, Malvern) and transmission electron microscopy (TEM) (Fei Tecnai F20 Super Twin TMP, ICN2) were used to determine particle distribution and size. TEM images were analyzed using ImageJ software to measure particle size. Atomic absorption spectroscopy was employed to determine silver nanoparticle concentration in solution and verify the reproducibility of

the synthesis.

2.3. Surface modification of endotracheal tubes

The reagents used for this procedure included m-phenylenediamine and cysteamine (Sigma-Aldrich, Merck), 98 % pure trimesoyl chloride (Alfa Aesar, Thermo Fisher Scientific), hexane, and ethanol (Pan Reac Appli Chem ITW reagents).

Segments of 6 mm diameter commercial polyvinyl chloride (PVC) endotracheal tubes were immersed in a solution of 2 g m-phenylenediamine and 98 mL distilled water for 3 minutes. Subsequently, they were immersed in a solution of 50 μ L 98 % pure trimesoyl chloride and 76 mL pure hexane for 30 seconds to form a thin polyamide (PA) film on the PVC surface. Excess materials were removed by washing with pure ethanol, followed by immersion in a 77.15 mg cysteamine and 50 mL distilled water solution for 4 hours to introduce thiol (SH) groups onto the surface. The samples were then immersed in a 50 mL solution of silver nanoparticles (AgNPs) for 24 hours to covalently bind the nanoparticles to the thiol groups on the PVC surface [22]. The immersion in the AgNPs solution was done at three concentrations: mother solution (100 %), diluted to 75 %, and 50 %. All procedures were conducted using an orbital shaker at 180 rpm.

2.4. Characterization of surface-modified endotracheal tubes

Scanning electron microscopy (SEM) (ZEISS Model EVO10 with EDS detector) was employed to assess the presence of immobilized nanoparticles on the PVC surface before and after the immobilization process, providing a semi-quantitative analysis of chemical composition. Surface chemical changes were determined using Fourier-transform infrared spectroscopy (FTIR) (PerkinElmer Spectrum TWO) in the 400–4000 cm^{-1} range and 24 scan cycles. Surface changes were analyzed by measuring the contact angle using an optical contact angle system (Dataphysics OCA 15EC) with 0.5 μ L distilled water droplets to confirm the success of the chemical modification and subsequent AgNPs immobilization.

The AgNPs-modified endotracheal tube segments at the three AgNPs concentrations were examined for antibacterial activity using agar diffusion assays. ATCC (American Type Culture Collection) strains of bacteria, *Klebsiella pneumoniae* ATCC 10031 and *Pseudomonas aeruginosa* ATCC 47085 were used. Bacteria were grown in agar plates at 37 °C for 24 hours. The antibacterial sensitivity method was employed with pure bacterial cultures adjusted to the McFarland 0.5 standard in agar Muller–Hinton. Unmodified PVC was used as the negative control, and five samples were tested for each AgNPs concentration. The samples were incubated at 37 °C for 24 hours and the inhibition zone diameter was measured.

Additionally, tensile strength was evaluated using a universal testing machine (SHIMADZU AGX 50KN, Shimadzu Analytical), this assay was based on the ASTM D638–22 standard, with a 5-ton load cell at a 50 mm/min speed. Rectangular tube segments measuring 80 mm in length, 10 mm in width, and 2 mm in thickness were cut for the test. The test was performed in triplicate for unmodified PVC tube segments and segments with AgNPs from the mother solution immobilized on their surface.

The cytotoxicity of the AgNPs-modified endotracheal tube segments was evaluated using fibroblast mouse cell line L929. The assessment followed ISO 10993–5:2009 standards, with untreated cells as the negative control and cells treated with medium containing dimethyl sulfoxide (DMSO) as the positive control. The samples were sterilized with ethylene oxide and incubated in fibroblast proliferation medium for 24 hours. The assay used 10,000 cells per well in 96-well plates and incubated them at 37 °C with 5 % CO_2 . After 24 hours, the cells were exposed to extracts from the modified samples for 24 hours. The MTT (3-[4,5-dimethylthiazol-2-yl]-2,5 diphenyl tetrazolium bromide) assay was then performed, with cytotoxicity expressed as a percentage of viable

cells relative to untreated cells.

3. Results and discussion

3.1. Synthesis of silver nanoparticles (AgNPs)

According to what is reported in the literature, a variety of colorations can be found for the synthesis of AgNPs nanoparticles, ranging from yellowish to bluish hues, which is associated with a change in the solution concentration [21,23]. During the process, a color change from transparent to yellow was observed, which is consistent with previous literature and indicates the successful formation of silver nanoparticles [21,24,25], using the developed methodology resulted in highly reproducible outcomes.

The concentration results measure for atomic absorption spectroscopy in three synthesized AgNPs solutions indicate an average value of 86.97 ± 2 mg Ag/L solution. This value demonstrates a high level of reproducibility of the chemical synthesis method because the concentration values obtained are close.

3.2. Characterization of silver nanoparticles (AgNPs)

3.2.1. Ultraviolet-Visible spectroscopy (UV-Vis)

In previous studies, it has been reported that the color-scheme of solution obtained for AgNPs will be associated with a wavelength value for the UV–vis spectrum, for nanoparticles exhibiting a yellowish tonality, the peak of maximum absorbance for colloids is in the range of 420–450 nm. These changes in the tonality and in the wavelength ranges depend on the method by which the AgNPs are synthesized, and this influences the size, shape, concentration, and agglomeration state of the particles [23,24,26].

Fig. 1 shows the UV-Vis spectrum obtained, revealing a peak of maximum absorbance at 417 nm. This peak falls within the range of 420–450 nm, typical of the surface plasmon resonance peak, confirming the formation of AgNPs. This finding agrees with literature reports [21, 27].

3.2.2. Dynamic light scattering (DLS)

Fig. 2 displays the size distribution obtained from analyzing the AgNPs mother solution using dynamic light scattering (DLS). Three graphs are presented for a single solution, corresponding to three detectors positioned at different angles (backscattering, side-scattering, and forward-scattering). The DLS results reveal that 87.48 % of AgNPs exhibit a size of 66.89 nm, while 18.78 % report a size of 11 nm. This intensity-based size distribution graph shows two main peaks for the reported particle sizes.

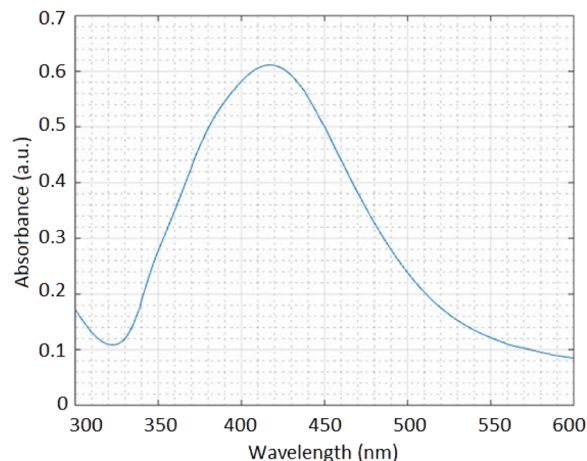


Fig. 1. UV-Vis spectroscopy of silver nanoparticles.

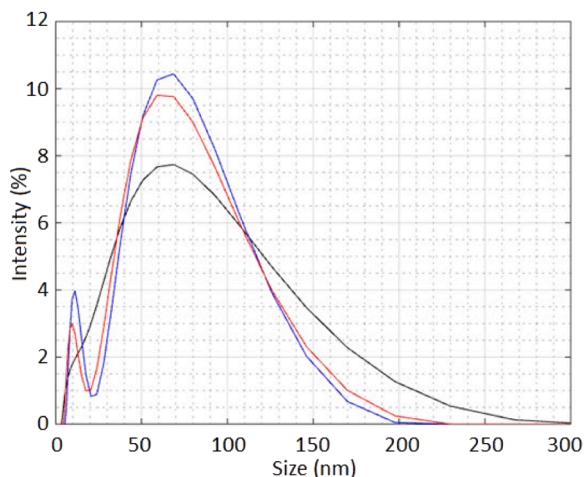


Fig. 2. Intensity-based size distribution.

The polydispersity index (PDI) of AgNPs synthesized was 0,44, this value indicates that the sample is highly polydisperse in size; this index is used to estimate the average uniformity of a particle solution, when and PDI values is high, there is a larger size distribution in the particle sample; and it is also possible than PDI high indicate the formation of nanoparticle aggregates. Agglomeration occurs because AgNPs possess low electrostatic charges on their surfaces, which are insufficient to effectively promote repulsion between nanoparticles [12]. A particle solution is considered monodisperse when the PDI value is less than 0.1 [28]. As reported in the literature, the obtained polydispersity is attributed to the role of trisodium citrate used as a reducing agent in the AgNPs synthesis. Trisodium citrate tends to generate a wide range of particle sizes and shapes within a single reaction [25,27].

3.2.3. Transmission Electron microscopy (TEM)

The TEM micrographs in Fig. 3 also show that the nanoparticles exhibit a pseudo-spherical geometry. Nguyen *et al.* [29] compared silver nanoparticles in the forms of rods, triangles, and spheres, finding that spherical AgNPs possess the strongest antibacterial activity and the most biocompatible characteristics. The pseudo-spherical AgNPs obtained in this work are close to spherical, suggesting the potential for good performance in antibacterial assays.

The TEM results revealed individual nanoparticles, allowing for measuring the size of approximately 60 particles using Image J software. It is important to note that the micrographs show an average size. However, there are also particles smaller than the average size, as evident in Fig. 3b, where smaller particles are visible. From the results

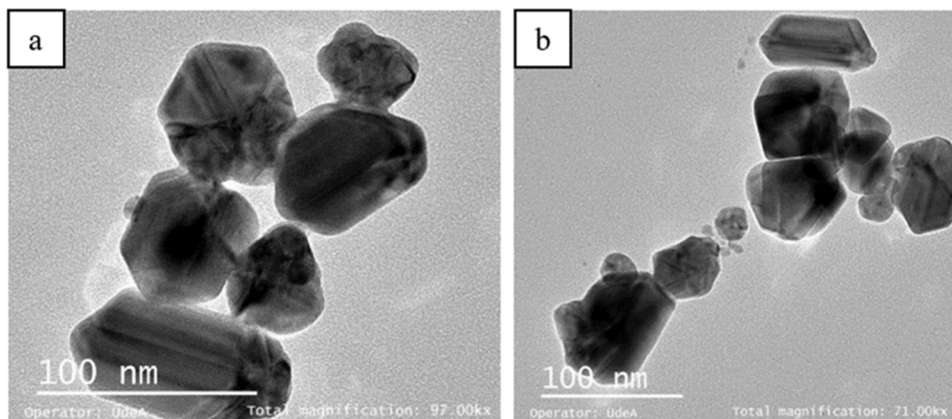


Fig. 3. TEM micrograph of synthesized silver nanoparticles.

presented in Fig. 4 and after measure 60 particles, most particles fall within the range of approximately 60–70 nm. The average size of these 60 measurements is calculated to be 59.67 nm, which closely corresponds to the value in the normal distribution. This value also closely matches the size obtained through the DLS analysis (66.89 nm).

3.3. Characterization of surface-modified endotracheal tubes

In Fig. 5, images of portions of commercial PVC tubes after chemical surface modification and subsequent immobilization of AgNPs are submitted.

The surface modification reveals that the initially transparent portions of PVC tubes (Fig. 5a) take on a translucent appearance with a yellow-brown hue (Fig. 5b, c, and d), characteristic of AgNPs, indicating successful immobilization of AgNPs on the surface [1,30]. Furthermore, it is evident that as the concentration of the AgNPs solution used for modification increases, the yellow tint becomes more intense on the samples, suggesting greater adherence of AgNPs to the surface.

3.3.1. Scanning electron microscopy (SEM)

Fig. 6 shows SEM micrographs of the endotracheal tube surfaces before and after AgNPs immobilization on the PVC surface. Before AgNPs immobilization, the PVC sample surface appears smooth (Fig. 6a). At the same time, after modification, significant deposition of AgNPs is evident (Fig. 6b, c, and d), along with the formation of nanoparticle agglomerates. This is a common phenomenon in nanostructured materials, where secondary and van der Waals bonds lead to particle

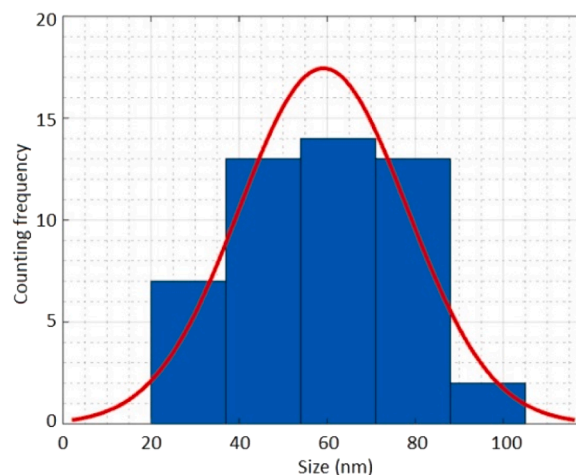


Fig. 4. Histogram of the 60 measurements performed on the sample AgNPs.

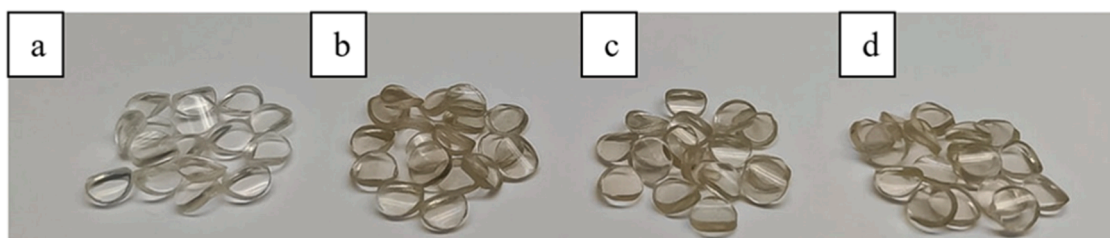


Fig. 5. Immobilization of AgNPs on endotracheal tube portions. (a) Unmodified PVC, (b) PVC - mother solution, (c) PVC - AgNPs 75 %, (d) PVC - AgNPs 50 %.

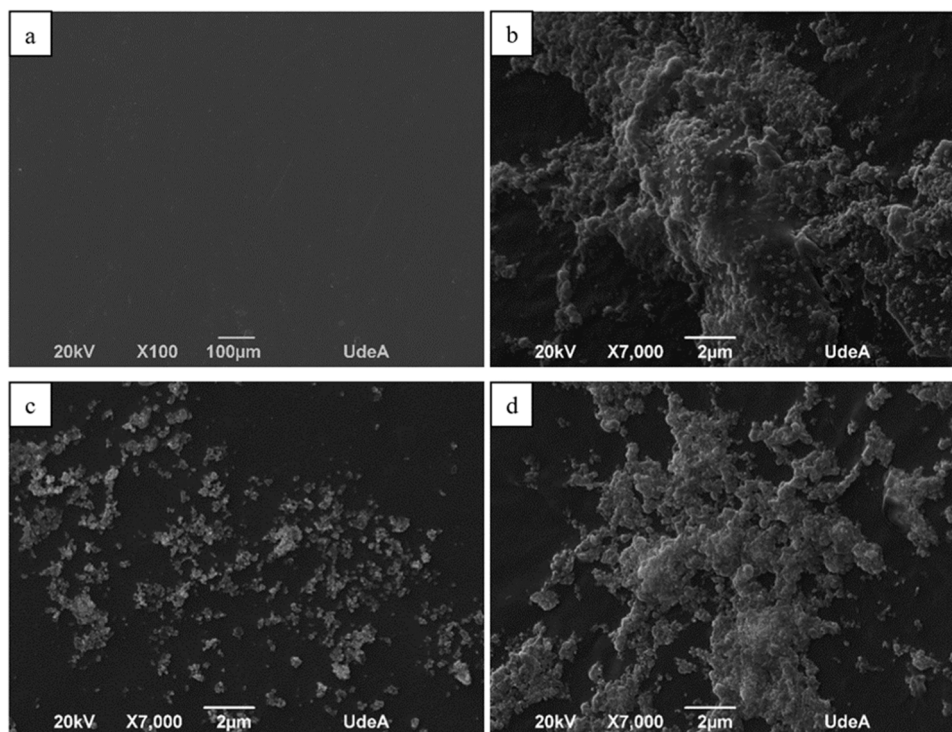


Fig. 6. SEM Micrograph. (a) PVC, (b) PVC - mother solution, (c) PVC - AgNPs 75 %, (d) PVC - AgNPs 50 %.

clustering to minimize energy states [31]. The surface is like that obtained by Yin *et al.* [30], who used a similar procedure to coat AgNPs on another substrate: polysulfone. The nanoparticles are distributed homogeneously over the entire surface of the material.

3.3.2. Fourier transform infrared spectroscopy (FTIR)

Fig. 7 displays the spectra obtained for the analyze the chemical composition of the PVC tube surface at each stage of the surface modification process and subsequent AgNPs immobilization.

For unmodified PVC, the spectrum confirms the presence of chlorinated hydrocarbons, with distinctive C-Cl peaks observed between 600 and 650 cm^{-1} . Additional peaks between 1000 and 1100 cm^{-1} correspond to C-C bonds, and the terminal CH_3 peak is between 1400 and 1425 cm^{-1} . Peaks between 2910 and 2970 cm^{-1} correspond to the asymmetric stretching mode of the terminal CH_2 . These findings agree with the literature regarding PVC [1,32].

The Fig. 7 spectrum reveals additional peaks after polyamide film formation (PVC-PA) between 1450 and 1650 cm^{-1} , including a peak around 1650 cm^{-1} indicative of amide I vibrations (C=O stretching). The peak at 1610 cm^{-1} signifies N-H stretching, and the peak at 1547 cm^{-1} corresponds to amide II vibrations (C-N stretching and N-H bending). The peak around 1450 cm^{-1} corresponds to C=O stretching and O-H bending of carboxylic acid. This fact confirms the formation of the PA film on the PVC surface [29,30,33–35].

A noticeable change between 3200 and 3600 cm^{-1} after PA film corresponds to the molecular vibration frequencies of N-H stretching. This result is attributed to the immersion of samples in cysteamine, which contains amine (N-H) and thiol (SH) functional groups in its structure. The AgNPs synthesized subsequently attach to the surface through Ag-S chemical bonds. Additionally, C=O and N-H functional groups present in AgNPs can prevent particle agglomeration and stabilize them in the medium [30,36,37].

Fig. 8 presents the spectrum obtained for PVC samples modified with different concentrations of AgNPs. After the immobilization process of AgNPs on PVC surfaces at different concentrations, it was observed that the peaks at 1547, 1610, and 1650 cm^{-1} , corresponding to the amide II, N-H, and amide I functional groups, decreased in intensity as the AgNPs concentration decreased. A peak at 1450 cm^{-1} was observed in the PVC-mother solution sample, which is not present in the samples with 75 % and 50 % AgNPs. Similarly, it is evident that in the region between 3200 and 3600 cm^{-1} corresponding to the amide (N-H) and thiol (SH) groups, the peak intensity is higher for the sample modified with the mother solution; conversely, for the other two concentrations, this peak is almost negligible. All the above confirms than changes are observed for the sample that was modified using the AgNPs mother solution.

3.3.3. Contact angle wetting assay

Table 1 presents the contact angle values for PVC surfaces with and

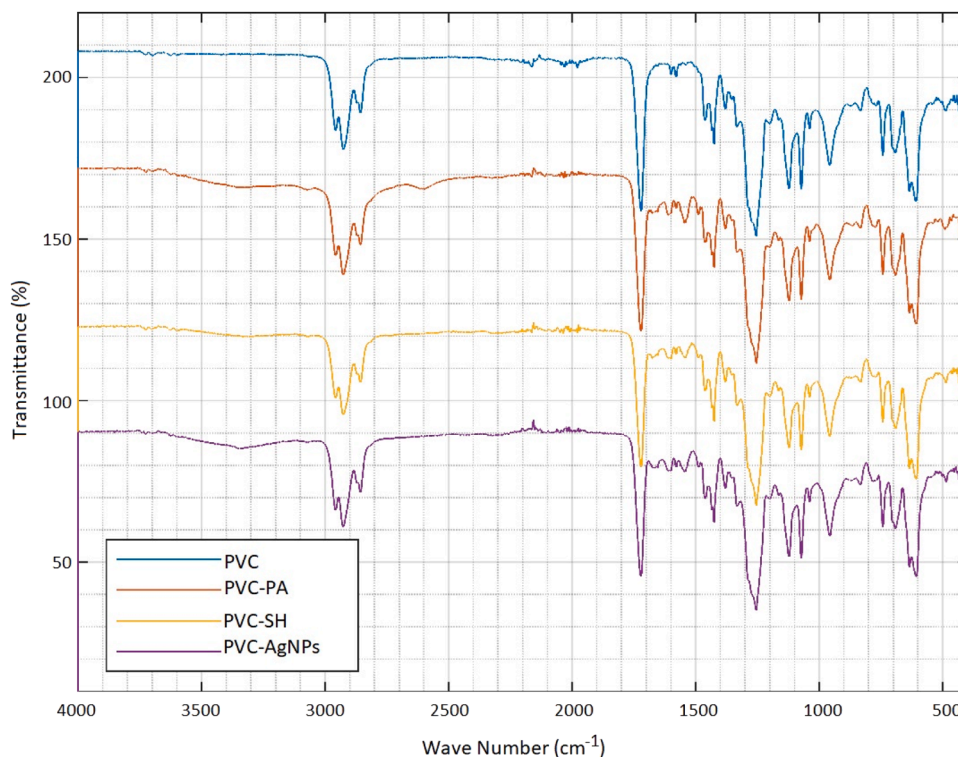


Fig. 7. FTIR spectrum of activated functional groups on PVC surface.

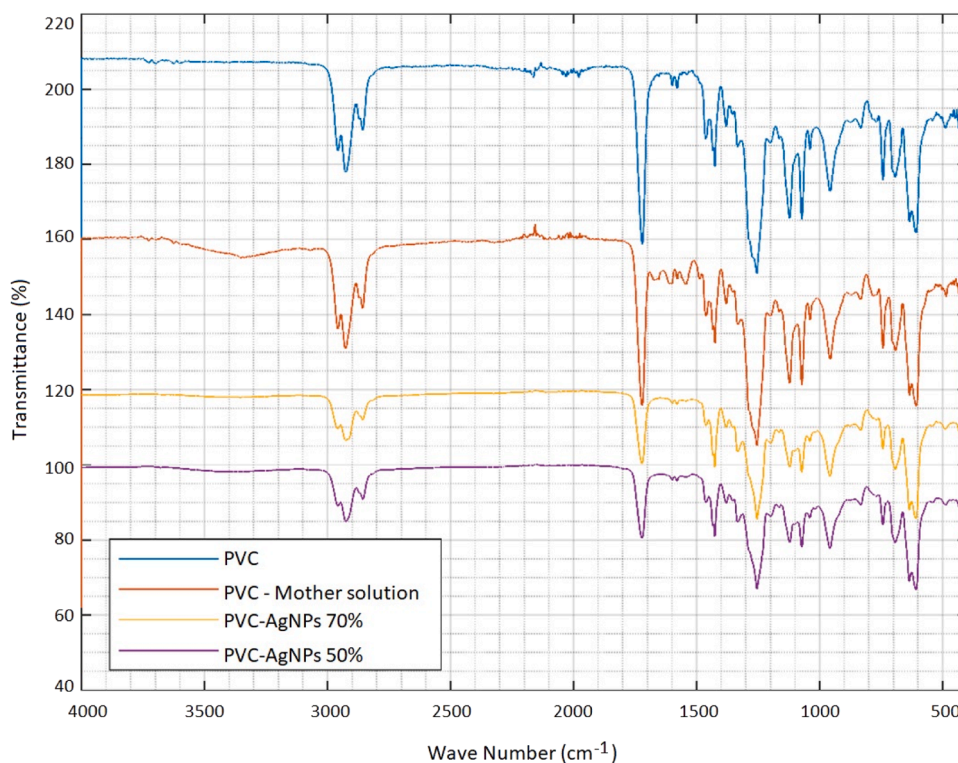
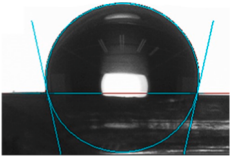
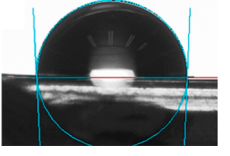
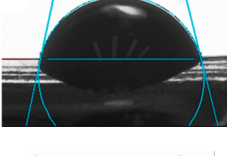
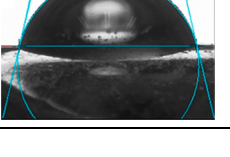


Fig. 8. FTIR spectra of PVC samples with different concentrations of AgNPs.

without modifications, along with images of distilled water droplets deposited on the material surface. As the AgNPs concentration increases, the liquid is drawn to the material and spreads across the surface. In contrast, unmodified PVC shows the highest angle due to surface hydrophobicity. The results confirm that the portions of PVC tubes before

AgNPs immobilization are hydrophobic, as evidenced by the 92.68° contact angle, similar value was measure for PVC by Wang *et al.* 2022 [12]. This finding corresponds with prior studies on medical-grade PVC surfaces [1]. It is notable that after AgNPs immobilization, the contact angle values decrease, and hydrophilicity is increased. The contact angle

Table 1
Water droplet on modified endotracheal tube surfaces.

Sample	Contact angle (°)	Water droplet
Unmodified PVC	92.68 ± 6.28	
PVC - AgNPs 50 %	90.68 ± 1.90	
PVC - AgNPs 75 %	83.10 ± 4.90	
PVC - mother solution	82.66 ± 5.30	

decreases as the AgNPs solution concentration used for modification increases. Metal nanoparticles have high surface energy [38]. In this study, AgNPs with an average size of 60 nm were used. When immobilized on PVC, they can increase the surface energy of the PVC, thereby decreasing the contact angle with water.

This change is attributed to AgNPs on the surface, increasing its polarity and turning it hydrophilic, thus reducing the contact angle. This fact is consistent with literature reports, the AgNPs accumulate on the surface, affecting its hydrophobicity directly [30,39–40]. This decrease in the contact angle does not affect the antimicrobial capacity of material, as will be discussed in the following item. Wang and colleagues achieved hydrophilic surfaces with contact angle values of 43° by coating PVC endotracheal tubes with a chitosan-AgNPs-gelatin mixture. This material exhibited suitable antibacterial properties to prevent ventilator-associated pneumonia [18]. Yin (2013) [30] observed a decrease in the contact angle for polysulfone membranes grafted with AgNPs due to the accumulation of AgNPs on the membrane surface. However, the material exhibited excellent antibacterial properties.

3.3.4. Antibacterial activity

The silver nanoparticles powerful antimicrobial effect is well known [41]. This study presented the inhibitory effect of the AgNPs against the two ATCC bacteria, these presented zones of inhibition that ranged between 7.1 mm and 7.6 mm (Table 2) against both analyzed strains, *Klebsiella pneumoniae* (Fig. 9) and *Pseudomonas aeruginosa* (Fig. 10), after incubation for 24 hours. The limited bactericidal effect was recognized when compared with the negative control (center sample) in the assays,

Table 2
Average inhibition zone for tested strains.

ATCC Strain	PVC – mother solution	PVC – AgNPs 75 %	PVC – AgNPs 50 %
<i>Klebsiella pneumoniae</i>	7.43 ± 0.53 mm	7.18 ± 0.16 mm	7.64 ± 0.60 mm
<i>Pseudomonas aeruginosa</i>	7.23 ± 0.76 mm	7.18 ± 0.48 mm	7.33 ± 0.65 mm

due to its growth inhibition did not occur.

Results show that, while all concentrations of AgNPs modifications exhibited inhibition zones, PVC - AgNPs 50 % showed an equal or larger inhibition zone than the mother solution against *Klebsiella pneumoniae*. This result aligns with the literature, as higher silver concentrations may lead to agglomeration on the surface, increasing particle size and decreasing diffusion efficiency, resulting in smaller inhibition zones [16].

The finding that *Pseudomonas aeruginosa* exhibited increased resistance to silver nanoparticles compared to *Klebsiella pneumoniae* presents interesting implications for its potential application in antimicrobial therapies. This disparity in susceptibility between the two bacterial species suggests that the efficacy of silver nanoparticles may vary depending on the target microorganism. The ability of *Pseudomonas aeruginosa* to resist the action of silver nanoparticles could be attributed to a series of factors, such as its innate resistance to antimicrobial agents and its ability to form protective biofilms [42]. It is important to note that these two strains are among the main pathogens colonizing the endotracheal tube surface, forming biofilms that can detach and migrate to the lung alveoli, causing pneumonia. Therefore, the results indicate the potential antibacterial activity of AgNPs against these strains.

This study was able to demonstrate a bactericidal effect of silver nanoparticles in PVC to enable their use in medical devices. Although the exact mechanism of action of silver nanoparticles is still not entirely clear [43]. Mechanisms described in the literature for the bactericidal effect of silver nanoparticles (AgNPs) include release of silver ions (Ag⁺) when they are in an aqueous medium. These ions can interact with sulfhydryl groups present in bacterial cell membranes, disrupt their structure and function, and cause bacterial cell death, this effect is fatal to Gram-negative bacteria, like *Pseudomonas aeruginosa*, as well as Gram-positive bacteria [44]. AgNPs can induce the formation of reactive oxygen species (ROS), such as hydrogen peroxide (H₂O₂) and hydroxyl radicals (OH), within bacterial cells. These reactive species can cause oxidative damage to essential cellular components, such as DNA, proteins and lipids, leading to bacterial cell death [45]. Also disrupting cellular function, AgNPs can interact directly with bacterial cell membranes, causing permeabilization and alteration of structural integrity. This can lead to loss of important cellular components and metabolic dysfunction, eventually leading to cell death. AgNPs can interfere with several vital cellular processes, such as protein synthesis and DNA replication, by interacting with cellular enzymes and proteins. This interference can trigger a cascade of events that lead to cell death [43].

Regarding the mechanism of action of AgNPs in inhibiting bacterial growth, the hypothesis is that AgNPs may contact bacterial cell membranes, disrupting their function due to strong bonding between AgNPs and the surface. Diffusion through the membrane might not be feasible, but contact could lead to membrane disruption, as reported by Yin *et al.* and Naaz *et al.* [30,46].

3.3.5. Mechanical strength

Table 3 presents the results after subjecting samples to the tensile strength test. The PVC - AgNPs sample exhibits greater deformation compared to unmodified PVC. However, overall, samples show similar stress and strain values.

The tensile strength does not differ before and after AgNPs immobilization, indicating that AgNPs do not influence the strength of material. Tensile properties of PVC can vary for effect of plasticizer, temperature, and crystallinity [11], nevertheless, in this work the processes implemented for the Ag immobilization, specifically chemical immersions had no effect on the material. The results are consistent with the literature [47,48]. For example, the tensile strength for PVC tube endotracheal evaluated for Wang *et al.* was 15 MPa approximately and the PVC coated with chitosan-AgNPs-gelatin do not have change in its mechanical resistance [18]. Instead, Da Silva *et al.* [12], in their research with PVC-AgNP (silver nanoparticles) material prepared through melt processing, founded significant differences in the tensile strength of PVC

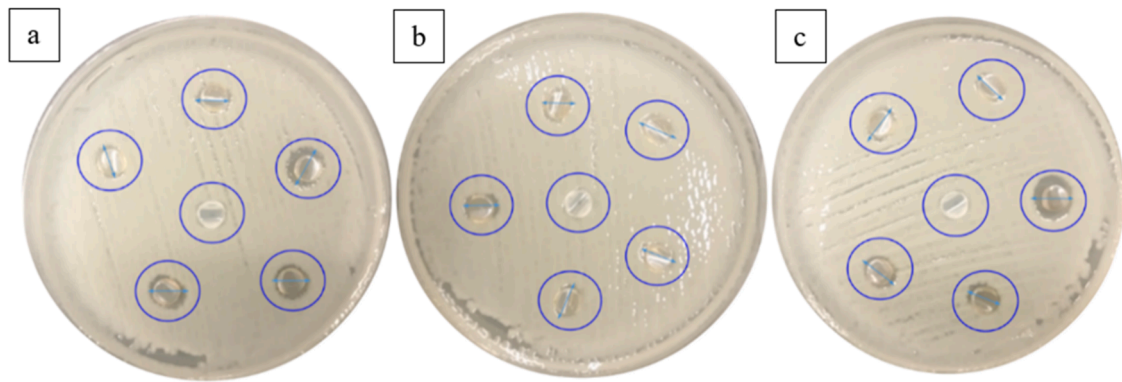


Fig. 9. Inhibition of *Klebsiella pneumoniae* growth on Trypto-Casein Soy Agar (TSA). (a) PVC - mother solution, (b) PVC - AgNPs 75 %, (c) PVC - AgNPs 50 %.

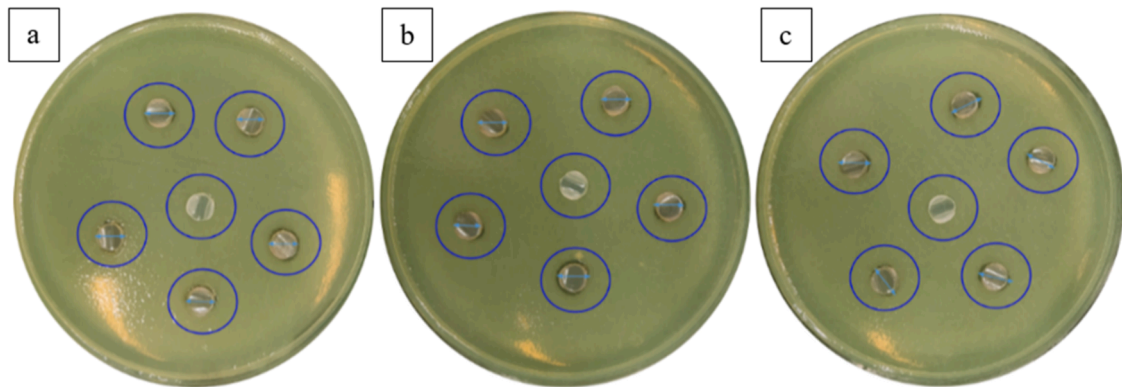


Fig. 10. Inhibition of *Pseudomonas aeruginosa* growth on Trypto-Casein Soy Agar (TSA). (a) PVC - mother solution, (b) PVC - AgNPs 75 %, (c) PVC - AgNPs 50 %.

Table 3

Average tensile strength test properties.

Material	Tensile Strength (MPa)	Rupture Deformation (%)
PVC	17.06 ± 3.01	148.19 ± 12.68
PVC – mother solution	16.30 ± 1.16	195.14 ± 36.66

respect to PVC-AgNP, this fact was explained due to that the AgNPs suspension reduces the interfacial adhesion between the PVC matrix with the inorganic microparticles, and there are poor stress transfer between these phases, causing a decrease of tensile strength for the material. In the present study the AgNPs are superficially, and they do not affect the mechanical properties.

It is important to note that endotracheal tubes remain stationary once inserted into the trachea of mechanically ventilated patients, so mechanical properties should not be a concern. However, there might be an effect due to the low oxygen pressure supplied to the patient, which could cause failure. Nonetheless, the obtained tensile strength demonstrates that the surface-modified endotracheal tubes are mechanically robust to prevent damage or fracture during intubation.

3.3.6. Cytotoxicity of PVC-AgNPs extracts on L929 cells

The cytotoxicity assay results are shown in Fig. 11. Results show no significant difference between unmodified PVC and PVC modified with the mother solution, with viability values around 80 %. The positive control result is as expected, with low cell viability when fibroblasts are incubated with DMSO-conditioned media, around 0 % viability. It is evident that the 10 % dilution AgNPs suspension, where AgNPs were not adhered to any material, exhibited cytotoxicity.

This behavior is due to the concentration of the AgNPs solution used to immerse PVC samples not necessarily being the final surface

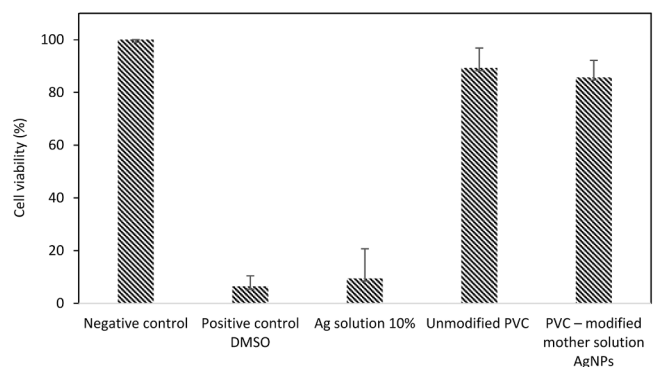


Fig. 11. Cell viability evaluated by MTT in L929 cells.

concentration, as it depends on the number of activated functional groups before AgNPs immobilization. Additionally, immobilizing AgNPs generates bonds that prevent nanoparticle migration to the medium, explaining why the aqueous AgNPs suspension displayed cytotoxicity while the solid PVC samples did not. This confirms that a water-based AgNPs suspension at a concentration of about 8.79 mg/L exhibits cytotoxicity on mouse fibroblast cells. PVC samples immobilized with AgNPs using the mother solution are not cytotoxic.

These results are comparable with previous studies, demonstrating that AgNPs exhibit lethal cytotoxicity at concentrations as low as 2–5 mg/L. However, they have also reported non-cytotoxic characteristics of AgNPs, even at high concentrations like 100 mg/L, due to factors such as coating types, particle size, and surface charge contributing to AgNPs toxicity [1,47]. It is necessary to verify the cytotoxic effects of each material configuration, as demonstrated in this study, where PVC

coated with AgNPs did not show adverse effects on cells. This fact is like obtaining by Wang [18] who were developed chitosan-AgNPs-gelatin nanocomposite coating on PVC, they evaluated the *in vitro* cytotoxicity in L929 cells and concluded that it is not toxic and suggesting that it could be safely used for coatings of endotracheal tubes.

According to the above, the samples with the highest concentration of AgNPs, mother solution, provided the ideal characteristics for the modification of endotracheal tubes, since they exhibited good stability of the immobilized nanoparticles and good antibacterial properties, without compromising the mechanical and non-cytotoxic properties of the material.

4. Conclusions

The formation of biofilms on materials used for manufacturing endotracheal tubes is the most widely accepted mechanism for the generation of pneumonia in patients with assisted breathing. In this work, silver nanoparticles (AgNPs) were successfully immobilized on commercial PVC tubes, this promising result suggests that surface modification with AgNPs offers a promising avenue for preventing VAP and enhancing patient safety during mechanical ventilation.

A methodology for the chemical synthesis of silver nanoparticles (AgNPs) was established, where AgNP stability was controlled by manipulating the temperature change at the end of the reaction. This approach prevented further growth over time, yielding an average size of 59.67 nm, obtained by TEM, suitable for potential surface modifications. The chemical synthesis process of AgNPs displayed high reproducibility, consistently yielding silver concentrations in the medium. These AgNPs were then immobilized on polyvinyl chloride (PVC) endotracheal tubes to enhance their antimicrobial properties.

Fourier-transform infrared spectroscopy (FTIR) and scanning electron microscopy (SEM) confirmed the presence of AgNPs on the PVC tube surface, validating the effectiveness of our modification process. The hydrophobic nature of commercial PVC tubes was altered through AgNPs immobilization, although the decrease in contact angle was observed (until 82.66° in PVC - mother solution material), this did not affect the antimicrobial properties of materials. The observed mechanical strength of the modified endotracheal tubes suggests that they conserved its mechanical integrity after Ag immobilization process, they are strong and stable for use in clinical settings, where they may be subjected to varying degrees of pressure and stress during intubation and mechanical ventilation procedures.

AgNPs-modified tubes demonstrated significant antibacterial activity against clinically relevant strains, including *Pseudomonas aeruginosa* and *Klebsiella pneumoniae*, they presented zones of inhibition that ranged between 7.1 mm and 7.6 mm. Additionally, they exhibited no cytotoxic effects on mouse fibroblast cells, indicating their safety for clinical application. This finding underscores the importance of ensuring patient safety while enhancing medical device functionality.

Future research should focus on clinical trials to validate the efficacy of AgNPs-modified endotracheal tubes in reducing VAP incidence and improving patient outcomes.

Author statement

The author of manuscript: IMMOBILIZATION OF SILVER NANOPARTICLES AT VARYING CONCENTRATIONS ON SEGMENTS OF POLYVINYL CHLORIDE MANUFACTURED ENDOTRACHEAL TUBES: Yesenia Andrea Murillo Arias, René Ramírez García, Marco Antonio González Agudelo, Nathalia Marín Pareja and Claudia Patricia Ossa Orozco, declare that in the preparation of this article we only use of basic tools for checking grammar, spelling, references.

CRedit authorship contribution statement

Claudia Patricia Ossa Orozco: Writing – review & editing,

Supervision, Project administration, Methodology, Investigation, Formal analysis, Conceptualization. Nathalia Marín Pareja: Writing – review & editing, Methodology, Investigation. René Ramírez García: Writing – review & editing, Investigation. Marco Antonio González Agudelo: Writing – review & editing, Investigation, Funding acquisition, Formal analysis, Conceptualization. Yesenia Andrea Murillo Arias: Writing – original draft, Methodology, Investigation, Formal analysis.

Declaration of Competing Interest

The authors declare that they have no known competing financial interests or personal relationships that could have appeared to influence the work reported in this paper.

Data availability

No data was used for the research described in the article.

Acknowledgement

The authors express their special appreciations to G8–2020 proyectos I+D+i: Desarrollo y validación de un nuevo diseño de neumotaponador integrado a un tubo orotraqueal que permite la prevención de la neumonía asociada a la ventilación mecánica en pacientes de cuidado intensivo - G8–2020 I+D+i projects: Development and validation of a new design of a pneumotaponador integrated to orotracheal tube that prevent of pneumonia associated with mechanical ventilation on intensive care patients.

References

- [1] C. Daengngam, S. Lethongkam, P. Srisamran, S. Paosen, P. Wintachai, B. Anantravanit, V. Vattanavanit, S. Voravuthikunchai, Green fabrication of antibacterial biofilm layer on endotracheal tubing using silver nanoparticles embedded in polyelectrolyte multilayered film, Mater. Sci. Eng. C 101 (2019) 53–63, <https://doi.org/10.1016/J.MSEC.2019.03.061>.
- [2] G. Ortiz, C. Duenas, M. Garay, Neumonía asociada a la ventilación mecánica: prevención, diagnóstico y tratamiento, Acta Colomb. Cuid. Intensivo 15 (4) (2015) 312–321, <https://doi.org/10.1016/J.ACCL.2015.09.006>.
- [3] M. Orozco-Levi, K. Pedrozo Arias, C. Pizarro Gómez, A. Ramírez-Sarmiento, El fracaso del efecto Pígalión para prevenir la broncoaspiración y sus complicaciones en pacientes intubados y ventilados mecánicamente, Acta Colomb. Cuid. Intensivo 21 (2) (2021) 152–160, <https://doi.org/10.1016/J.ACCL.2020.12.002>.
- [4] L.G. Bassi, N. Luque, J.D. Martí, E. Aguilera-Xiol, M. Di Pasquale, V. Giunta, T. Comaru, M. Rigol, S. Terraneo, F. De Rosa, M. Rinaudo, E. Crisafulli, R. C. Peralta-Lepe, C. Agusti, C. Lucena, M. Ferrer, L. Fernández, A. Torres, Endotracheal tubes for critically ill patients: an in vivo analysis of associated tracheal injury, mucociliary clearance, and sealing efficacy, Chest 147 (5) (2015) 1327–1335, <https://doi.org/10.1378/CHEST.14-1438>.
- [5] H.D. Spapen, E. Suys, M. Diltoer, W. Stiers, G. Desmet, P.M. Honoré, A newly developed tracheal tube offering ‘pressurised sealing’ outperforms currently available tubes in preventing cuff leakage: a benchtop study, Eur. J. Anaesthesiol. 34(7) (2107) 411–416, <https://doi.org/10.1097/EJA.0000000000000493>.
- [6] E. Jailllette, C. Girault, G. Brunin, F. Zerimech, H. Behal, A. Chiche, C. Brouqsault-Dedrie, C. Fayolle, F. Minacori, I. Alves, S. Barrailler, J. Labreuche, L. Robriquet, F. Tamion, E. Delaporte, D. Thellier, C. Delcourte, A. Duhamel, S. Nseir, Impact of tapered-cuff tracheal tube on microaspiration of gastric contents in intubated critically ill patients: a multicenter cluster-randomized cross-over controlled trial, Intensive Care Med. 43 (11) (2017) 1562–1571, <https://doi.org/10.1007/S00134-017-4736-X/TABLES/5>.
- [7] M. Busico, L. Vega, G. Plotnikow, N. Tiribelli, Tubos endotraqueales: revisión | Revista Argentina de Terapia Intensiva, Revista Argentina de Terapia Intensiva, (2013), (<https://revista.sati.org.ar/index.php/MI/article/view/341>) (Accessed 23 July 2021).
- [8] P. Schilardi, D. Pissinis, Tratamiento de la Neumonía Asociada a la Ventilación Mecánica: cofactor de mortalidad en pacientes COVID-19 positivos, Innovación. Y. Desarro. Tecnol. ógico Y. Soc. 2 (2) (2020) 118–133, <https://doi.org/10.24215/26838559E019>.
- [9] M.F. Ochoa Franco, Neumotaponador de tubo endotraqueal con inflado controlado a partir de una variable diferente a su presión interna, EIA Univerity. 2019. (Accessed 16 May 2024). (<https://repository.eia.edu.co/server/api/core/bitstream/2648a67e-f34b-4a65-8932-9712d465c97a/content>).

- [10] M.B. Serna, D. Paz, M.L. Mariscal, Descripción de los tubos endotraqueales, Anestesia.org, (2012), (<https://anestesiario.org/2012/descripcion-de-los-tubos-endo-traqueales/>) (Accessed 24 July 2021).
- [11] K.Z. Hong, Poly(vinyl chloride) in medical device and packaging applications, *J. Vinyl Addit. Technol.* 2 (3) (1996) 193–197, <https://doi.org/10.1002/vnl.10123>.
- [12] D.J. da Silva, G.B. Gramscianinov, P.Z. Jorge, V.B. Malaquias, A.A. Mori, M. H. Hirata, S.A.M. Lopes, L.A. Bueno, M. Champeau, D.J. Carastan, PVC containing silver nanoparticles with antimicrobial properties effective against SARS-CoV-2, *Front. Chem.* 11 (2023) 1083399, <https://doi.org/10.3389/fchem.2023.1083399>.
- [13] J. Hasan, R.J. Crawford, E.P. Ivanova, Antibacterial surfaces: the quest for a new generation of biomaterials, *Trends Biotechnol.* 31 (5) (2013) 295–304, <https://doi.org/10.1016/j.tibtech.2013.01.017>.
- [14] A. Cano Melguizo, S.A. Castro Floréz, Evaluación de la adhesión bacteriana a la superficie de arcos de acero inoxidable de uso ortodóncico modificados siguiendo un enfoque biomimético (2019) (Accessed 16 May 2024). (<https://repository.ucc.edu.co/server/api/core/bitstreams/bafbc37-4275-4d56-8779-51ed4bae59a1/content>).
- [15] J. Osorio Echavarría, N.A. Gómez Vanegas, C.P. Ossa Orozco, Chitosan/carboxymethyl cellulose wound dressings supplemented with biologically synthesized silver nanoparticles from the ligninolytic fungus *Anamorphous Bjerkanthera sp. R1*, *Heliyon* 8 (2022) e10258, <https://doi.org/10.1016/j.heliyon.2022.e10258>.
- [16] L.R. Braga, E.T. Rangel, P.A.Z. Suarez, F. Machado, Simple synthesis of active films based on PVC incorporated with silver nanoparticles: evaluation of the thermal, structural and antimicrobial properties, *Food Packag. Shelf Life* 15 (2018) 122–129, <https://doi.org/10.1016/j.fpsl.2017.12.005>.
- [17] O. Dutta, A. Ficaí, and D. Ficaí O.C. Duñá, A. Ficaí, D. Ficaí, R.D. Truşcă, E. Grosu, L. M. Ditu, G. Mihăescu, M.C. Chifiriuc, E. Andronescu, PVC Modification by incorporating silver nanoparticles on the surface, *U.P.B. Sci. Bull., Ser. B*, 82(3) (2020) 85–100, (Accessed 16 May 2024) (https://www.scientificbulletin.upb.ro/rev_docs_arhiva/full24f_173087.pdf).
- [18] Y. Wang, B. Cai, D. Ni, Y. Sun, G. Wang, H. Jiang, A novel antibacterial and antifouling nanocomposite coated endotracheal tube to prevent ventilator-associated pneumonia, *J. Nanobiotechnol.* 20 (2022) 112, <https://doi.org/10.1186/s12951-022-01323-x>.
- [19] Ch. Ch Hu, Y. Yu, H.L. Qian, Y.F. Chen, L.Y. Zou, Ch.M. Zhang, K.F. Ren, Z.H. Yang, J. Ji, Antibacterial endotracheal tube with silver-containing double-network hydrogel coating, *Colloid Interface Sci. Commun.* 55 (2023) 100724, <https://doi.org/10.1016/j.colcom.2023.100724>.
- [20] M.F. Al-Sayed, M.T. El-Wakad, M.A. Hassan, A.M. Soliman, A.S. Eldesoky, optimal concentration and duration of endotracheal tube coating to achieve optimal antimicrobial efficacy and safety balance: an *in vitro* study, *Gels* 9 (2023) 414, <https://doi.org/10.3390/gels9050414>.
- [21] G. Cuervo Osorio, M. Escobar Jaramillo, C.P. Ossa Orozco, Diseño factorial 2k para la optimización de la síntesis de nanopartículas de plata para su aplicación en biomateriales, *Rev. ION* 33 (1) (2020) 17–32, <https://doi.org/10.18273/revion.v33n1-2020002>.
- [22] S. Maharubin, C. Nayak, O. Phatak, A. Kurhade, M. Singh, Y. Zhou, G. Tan, Polyvinylchloride coated with silver nanoparticles and zinc oxide nanowires for antimicrobial applications, *Mater. Lett.* 249 (2019) 108–111, <https://doi.org/10.1016/j.matlet.2019.04.058>.
- [23] F.M. Martínez, E. Zuñiga, A.K. Sánchez Lafarga, Método de síntesis de nanopartículas de plata adaptable a laboratorios de docencia relacionado con la nanotecnología, *Mundo nano. Rev. Interdiscip. En. nanociencias Y. nanotecnología* 6 (10) (2021) 101–108, <https://doi.org/10.22201/ceiich.24485691e.2013.10.50967>.
- [24] J.P. Gallo Ramírez, C.P. Ossa Orozco, Fabrication and characterization of silver nanoparticles with potential use in the treatment of skin cancer, *Ing. fa Y. Desarro.* 37 (1) (2019) 88–104, <https://doi.org/10.14482/inde.37.1.6201>.
- [25] L. Oprica, M. Andries, L. Sacarescu, L. Popescu, D. Priscop, D. Creanga, M. Balasoitu, Citrate-silver nanoparticles and their impact on some environmental beneficial fungi, *Saudi J. Biol. Sci.* 27 (12) (2020) 3365–3375, <https://doi.org/10.1016/j.sjbs.2020.09.004>.
- [26] S. Mourdikoudis, R.M. Pallares, N.T.K. Thanh, Characterization techniques for nanoparticles: comparison and complementarity upon studying nanoparticle properties, *Nanoscale* 10 (2018) 12871–12934, <https://doi.org/10.1039/c8nr02278j>.
- [27] M. Sánchez, Nanopartículas de plata: preparación, caracterización y propiedades con aplicación en inocuidad de los alimentos (2017). Accessed: May. 16, 2024. [Online]. Available: (http://e-spacio.uned.es/fez/eserv/bibliuned:mater-Ciencias-CyTQ-Msanchez/Sanchez_Moreno_Minerva_TFM.pdf).
- [28] K.N. Clayton, J.W. Salameh, S.T. Wereley, T.L. Kinzer-Ursem, Physical characterization of nanoparticle size and surface modification using particle scattering diffusometry, *Biomicrofluidics* 10 (5) (2016) 054107, <https://doi.org/10.1063/1.4962992>.
- [29] D.D. Nguyen, L.J. Luo, J.Y. Lai, Toward understanding the purely geometric effects of silver nanoparticles on potential application as ocular therapeutics via treatment of bacterial keratitis, *Mater. Sci. Eng.: C* 119 (2021) 111497, <https://doi.org/10.1016/j.msec.2020.111497>.
- [30] J. Yin, Y. Yang, Z. Hu, B. Deng, Attachment of silver nanoparticles (AgNPs) onto thin-film composite (TFC) membranes through covalent bonding to reduce membrane biofouling, *J. Memb. Sci.* 441 (2013) 73–82, <https://doi.org/10.1016/j.memsci.2013.03.060>.
- [31] M. Gómez-Garzón, Nanomateriales, Nanopartículas y Síntesis verde, *Rev. Repert. De. Med. Y. Cirugía* 27 (2) (2018), <https://doi.org/10.31260/RepertMedCir.v27.n2.2018.191>.
- [32] M. Pandey, G.M. Joshi, A. Mukherjee, P. Thomas, Electrical properties and thermal degradation of poly(vinyl chloride)/polyvinylidene fluoride/ZnO polymer nanocomposites, *Polym. Int.* 65 (9) (2016) 1098–1106, <https://doi.org/10.1002/Pl.5161>.
- [33] P. Poletto, J. Duarte, M.S. Lunkes, V. dos Santos, M. Zeni, C.S. Meireles, G. R. Filho, A. Bottino, Avaliação das características de transporte em membranas de poliamida 66 preparadas com diferentes solventes, *Polímeros* 22 (3) (2012) 273–277, <https://doi.org/10.1590/S0104-14282012005000041>.
- [34] V.M. Ndesendo, Y.E. Choonara, L.C. Meyer, P. Kumar, L.K. Tomar, C. Tyagi, L.C. du Toit, V. Pillay, *In vivo* evaluation of a mucoadhesive polymeric caplet for intravaginal anti-HIV-1 delivery and development of a molecular mechanistic model for thermochemical characterization, *Drug Dev. Ind. Pharm.* 41 (8) (2015) 1274–1287, <https://doi.org/10.3109/03639045.2014.947506>.
- [35] R.D. Munje, S. Muthukumar, B. Jagannath, S. Prasad, A new paradigm in sweat based wearable diagnostics biosensors using Room Temperature Ionic Liquids (RTILs), *Sci. Rep.* 7 (1) (2017), <https://doi.org/10.1038/S41598-017-02133-0>.
- [36] N. Golla, J.M.A. Alzohairy, H. Khadri, K. Mallikarjuna, Extracellular synthesis, characterization and antibacterial activity of silver nanoparticles by *Actinomyces isolative*, *Int. J. Nano Dimens.* 4 (1) (2013) 77–83, <https://doi.org/10.7558/IJND.2013.01.010>.
- [37] A.O. Akintola, B.D. Kehinde, P.B. Ayoola, A.G. Adewoyin, O.T. Adedosu, J.F. Ajayi, S.B. Ogunsona, Antioxidant properties of silver nanoparticles biosynthesized from methanolic leaf extract of *Blighia sapida*, *IOP Conf. Ser. Mater. Sci. Eng.* 805 (1) (2020), <https://doi.org/10.1088/1757-899X/805/1/012004>.
- [38] S. Kasraei, M. Azarsina, Addition of silver nanoparticles reduces the wettability of methacrylate and silorane-based composites, *Braz. Oral. Res.* 26 (6) (2012) 505–510, <https://doi.org/10.1590/S1806-83242012000600004>.
- [39] L. Esteban, Actividad biocida de vidrios sodocálcicos conteniendo nanopartículas de plata o cobre. 2012. Accessed May 16, 2024. [Online]. Available: (<https://dialnet.unirioja.es/servlet/tesis?codigo=32746&msckid=ca068fb7bd8d11ebc22341>) 4bb92710b7.
- [40] L. Muñoz Jiménez, Estudio del efecto de la incorporación superficial de nanopartículas de plata sobre las propiedades físicas y antimicrobianas de películas multicapa y oxodegradables. 2016. (Accessed 16 May 2024). (<https://ciqa.repositorioinstitucional.mx/jspui/handle/1025/563>).
- [41] Y.G. Yuan, Q.L. Peng, S. Gurunathan, Effects of silver nanoparticles on multiple drug-resistant strains of *Staphylococcus aureus* and *Pseudomonas aeruginosa* from mastitis-infected goats: an alternative approach for antimicrobial therapy, *de 2017*, *Int. J. Mol. Sci.* 18 (3) (2017) 569, <https://doi.org/10.3390/ijms18030569>.
- [42] D. de Lacerda Coriolano, J.B. de Souza, E.V. Bueno, Sa.M.F. Ramos dos Santos Medeiros, I.D. Lima Cavalcanti, I.M. Ferro Cavalcanti, Antibacterial and antibiofilm potential of silver nanoparticles against antibiotic-sensitive and multidrug-resistant *Pseudomonas aeruginosa* strains, *Braz. J. Microbiol.* 52 (1) (2021) 267–278, <https://doi.org/10.1007/s42770-020-00406-x>.
- [43] N. Durán, M. Durán, M.B. de Jesus, A.B. Seabra, W.J. Fávoro, G. Nakazato, Silver nanoparticles: a new view on mechanistic aspects on antimicrobial activity, *Nanomед. Nanotechnol. Biol. Med* 12 (3) (2016) 789–799, <https://doi.org/10.1016/j.nano.2015.11.016>.
- [44] D.J. Balazsa, K. Triandafillub, P. Wood, Y. Chevoluta, C. van Deldenc, H. Harmsb, C. Hollensteind, H.J. Mathieu, Inhibition of bacterial adhesion on PVC endotracheal tubes by RF-oxygen glow discharge, sodium hydroxide and silver nitrate treatments, *Biomaterials* 25 (2004) 2139–2151, <https://doi.org/10.1016/j.biomaterials.2003.08.053>.
- [45] Y.N. Slavin, J. Asnis, U.O. Häfeli, H. Bach, Metal nanoparticles: understanding the mechanisms behind antibacterial activity, *J. Nanobiotechnol.* 15 (2017) 65, <https://doi.org/10.1186/s12951-017-0308-z>.
- [46] R. Naaz, V.U. Siddiqui, S.U. Qadir, W.A. Siddiqi, Green synthesis of silver nanoparticles using *Syngonium podophyllum* leaf extract and its antibacterial activity, *Mater. Today Proc.* 46 (2021) 2352–2358, <https://doi.org/10.1016/J.MATPR.2021.05.062>.
- [47] C.Y. Loo, P.M. Young, W.H. Lee, R. Cavaliere, C.B. Whitchurch, R. Rohanizadeh, Non-cytotoxic silver nanoparticle-polyvinyl alcohol hydrogels with anti-biofilm activity: designed as coatings for endotracheal tube materials, *Biofouling J. Bioadhesion Biofilm Res.* 30 (7) (2014) 773–788, <https://doi.org/10.1080/08927014.2014.926475>.
- [48] R.S. Jones, J.G. McGovern, A.D. Woolfson, C.G. Adair, S.P. Gorman, Physicochemical characterization of hexetidine-impregnated endotracheal tube poly(vinyl chloride) and resistance to adherence of respiratory bacterial pathogens, *Pharm. Res.* 19 (6) (2002) 818–824, <https://doi.org/10.1023/A:1016104516034>.